Video Article

High Resolution Physical Characterization of Single Metallic Nanoparticles

Jessica Ettedgui[1,2], Jacob Forstater[1,2], Joseph W. Robertson[1], John J. Kasianowicz[1,3]

[1]Physical Measurement Laboratory, National Institute of Standards and Technology

[2]Department of Chemical Engineering, Columbia University

[3]Department of Applied Physics and Applied Math, Columbia University

Correspondence to: Jessica Ettedgui at jessicaettedgui@gmail.com

URL: https://www.jove.com/video/58257
DOI: doi:10.3791/58257

Keywords: Nanopore, α-Hemolysin, Lipid bilayer, Single-molecule analysis, Polyoxometalates, Isomers

Date Published: 6/28/2018

Citation: Ettedgui, J., Forstater, J., Robertson, J.W., Kasianowicz, J.J. High Resolution Physical Characterization of Single Metallic Nanoparticles. *J. Vis. Exp.* (), e58257, doi:10.3791/58257 (2018).

Abstract

Individual molecules can be detected and characterized by measuring the degree by which they reduce the ionic current flowing through a single nanometer-scale pore. The signal is characteristic of the molecule's physicochemical properties and its interactions with the pore. We demonstrate that the nanopore formed by the bacterial protein exotoxin *Staphylococcus aureus* alpha hemolysin (αHL) can detect polyoxometalates (POMs, anionic metal oxygen clusters), at the single molecule limit. Moreover, multiple degradation products of 12-phosphotungstic acid POM (PTA, $H_3PW_{12}O_{40}$) in solution are simultaneously measured. The single molecule sensitivity of the nanopore method allows for POMs to be characterized at significantly lower concentrations than required for nuclear magnetic resonance (NMR) spectroscopy. This technique could serve as a new tool for chemists to study the molecular properties of polyoxometalates or other metallic clusters, to better understand POM synthetic processes, and possibly improve their yield. Hypothetically, the location of a given atom, or the rotation of a fragment in the molecule, and the metal oxidation state could be investigated with this method. In addition, this new technique has the advantage of allowing the real-time monitoring of molecules in solution. The single molecule sensitivity of the nanopore method allows for POMs to be characterized at significantly lower concentrations than required for NMR spectroscopy and other techniques.

Introduction

Detecting biomolecular analytes at the single molecule level can be performed by using nanopores and measuring ionic current modulations. Typically, nanopores are divided into two categories based on their fabrication: biological (self-assembled from protein or DNA origami)[1,2,3], or solid-state (*e.g.*, manufactured with semiconductor processing tools)[4,5]. While solid-state nanopores were suggested as potentially more physically robust and offer a wide range of solution conditions, protein nanopores thus far offer greater sensitivity, more resistance to fouling, greater bandwidth, better chemical selectivity, and a greater signal to noise ratio.

A variety of protein ion channels, such as the one formed by *Staphylococcus aureus α*-hemolysin (αHL), can be used to detect single molecules, including ions (*e.g.*, H^+ and D^+)[2,3], polynucleotides (DNA and RNA)[6,7,8], damaged DNA[9], polypeptides[10], proteins (folded and unfolded)[11], polymers (polyethylene glycol and others)[12,13,14], gold nanoparticles[15,16,17,18,19], and other synthetic molecules[20].

We recently demonstrated that the αHL nanopore can also easily detect and characterize metallic clusters, polyoxometalates (POMs), at the single molecule level. POMs are discrete nanoscale anionic metal oxygen clusters that were discovered in 1826[21], and since then, many more have been synthesized. The different sizes, structures, and elemental compositions of polyoxometalates that are now available led to a wide range of properties and applications including chemistry[22,23], catalysis[24], material science[25,26], and biomedical research[27,28,29].

POM synthesis is a self-assembly process typically carried out in water by mixing the stoichiometrically required amounts of monomeric metal salts. Once formed, POMs exhibit a great diversity of sizes and shapes. For example, the Keggin polyanion structure, $XM_{12}O_{40}^{q-}$ is composed of one heteroatom (X) surrounded by four oxygens to form a tetrahedron (q is the charge). The heteroatom is centrally located within a cage formed by 12 octahedral MO_6 units (where M = transition metals in their high oxidation state), which are linked to one another by neighboring shared oxygen atoms. While tungsten polyoxometalates structure is stable in acidic conditions, hydroxide ions lead to the hydrolytic cleavage of metal-oxygen (M-O) bonds[30]. This complex process results in the loss of one or more MO_6 octahedral subunits, leading to the formation of monovacant and trivacant species and eventually to the complete decomposition of POM. Our discussion here will be limited to the partial decomposition products of 12-phosphotungstic acid at pH 5.5 and 7.5.

The goal of this protocol is to detect discrete metal oxygen clusters at the single molecule limit using a biological nanopore-based electronic platform. The nanopore-based analytical method allows the detection of metallic clusters in solution. Multiple species in solution can be discriminated with greater sensitivity than conventional analytical methods[33]. With it, subtle differences in POM structure can be elucidated, and at concentrations markedly lower than those required for NMR spectroscopy. Importantly, this approach even allows the discrimination of isomeric forms of $Na_8HPW_9O_{34}$[1].

Copyright © 2018 Journal of Visualized Experiments

Protocol

Note: The protocol below is specific to the Electronic BioSciences (EBS) Nanopatch DC System. However, it can be readily adapted to other electrophysiology apparatus used to measure the current through planar lipid bilayer membranes (standard lipid bilayer membrane chamber, U-tube geometry, pulled microcapillaries, *etc.*). The identification of commercial materials and their sources is given to describe the experimental results. In no case does this identification imply recommendation by the National Institute of Standards and Technology, nor does it imply that the materials are the best available.

1. Solution and Analyte Preparation

1. Prepare all electrolyte solutions with 18 MΩ-cm water from a Type-1 water purification system to remove trace organic species and then filter all electrolyte solutions through a 0.22 µm vacuum filter immediately before ion channel recordings.
   Note: The water quality is a critical factor for the stability and longevity of the membrane nanopore system.
2. Wild Type αHL.
   1. Follow MSDS precautions when handling the αHL toxin protein.
   2. Mix lyophilized wild-type monomeric *S. aureus α*-Hemolysin (*α*HL) powder with 18 MΩ-cm water at 1 mg/mL. Distribute 10 to 30 µL aliquots of the sample into cryo-safe centrifuge tubes, quickly flash freeze in liquid nitrogen and then store at -80 °C. Alternatively, use purified preformed heptameric *α*HL[31].
3. Dissolve the lipid 1,2-Diphytanoyl-sn-Glycero-3-Phosphocholine (DPhyPC) to 0.2 mg/mL in *n*-decane in a 4 mL glass scintillation vial with a polytetrafluoroethyleneeflon-coated cap. Store the solution at 4 °C for repeated use for up to one month.
4. Prepare phosphotungstic acid solutions.
   1. Prepare a 2 mM phosphotungstic acid stock solution by dissolving 57.6 mg of $H_3PW_{12}O_{40}$ into 10 mL of a 1 M NaCl and 10 mM NaH_2PO_4 solution, which constitutes the stock solution.
   2. Take 5 mL of this solution and adjust the pH to 5.5 with 3 M NaOH. Adjust the pH of the other 5 mL of the stock solution to 7.5 with 3 M NaOH.
      Note: At pH 5.5, 12-phosphotungstic acid (PTA, $H_3PW_{12}O_{40}$) decomposes primarily into the monovacant anion $[PW_{11}O_{39}]^{7-}$.

2. Test Cell Assembly

1. Assemble the test cell per the manufacturer's instructions.
2. Soak one Ag/AgCl wire in bleach (sodium hypochlorite) for 10 minutes after abrading it with 600 grit sandpaper. Position the electrode inside the quartz nanopore membrane (QNM).
3. Place a cylindrical AgCl pellet electrode embedded in a silver wire outside of the QNM.
4. Once the test cell is set up, turn on the power supply and data acquisition program. Ensure that the DC current reading is 0 pA in the absence of solution in the test cell.
5. Use a syringe connected to the test cell *via* a fluid line to add buffered electrolyte solution above the face of the QNM and to ensure that the ionic current saturates the amplifier. If it does not, the QNM may be clogged. Apply a pop voltage (± 1 V) and/or a pressure greater than 300 mm Hg to clear it. If that works, reduce the voltage and pressure.

3. Lipid Bilayer Formation

1. Fill the solution in the test cell so that the solution level is well above the face of the QNM. Then lower the solution level *via* syringe to below the face, such that the current decreases to zero.
2. Dip a 10 µL pipette tip into the lipid vial. Push on the back end of the pipette tip and tap it on the side of the vial to remove all visible lipid.
3. Touch the pipette tip onto the air-water interface of the solution in the test cell when the solution level is above the QNM's face and wait two to five minutes for the lipid to spread uniformly.
4. Slowly lower the solution level below the face of the QNM until the current saturates, and then slowly raise the solution level past the face of the QNM to form a lipid bilayer membrane.
   1. Once a bilayer appears to form (*i.e.,* when the current goes to zero), try popping it several times by increasing the pressure and ensure that the QNM is not clogged. To reform the lipid bilayer membrane, lower again the solution level below the face of the QNM and slowly raise it.
5. If the lipid bilayer membrane did not form the first time, lower the solution below the face and raise it again. If it does not form after 3 trials, add some lipids again as described in 3.2 and 3.3.
6. After forming a membrane, set the current offset to zero when the applied potential is zero.

4. *α*HL Pore Formation

1. Add 2.5 ng of purified preformed *α*HL heptameric protein sample to the test cell (volume ≈ 200 µL) to enable insertion of the protein or alternatively 250 ng of monomeric αHL.
2. Increase the pressure on the bilayer with a gas-tight syringe (**Figure 1**) after a bilayer is formed, to expand the membrane from the QNM, and facilitate nanopore insertion. Raise the applied back pressure typically between 40 to 200 mmHg, depending on each QNM.
   Note: The EBS software has an automated insertion feature that applies a higher bias (typically 200 to 400 mV) to induce pore formation and then automatically reduces the desired voltage to the measurement bias once a single channel forms.

3. After a nanopore forms, reduce the back-pressure to about 1⁄2 of the insertion pressure. If multiple channels are observed, remove them by significantly reducing the pressure.

5. Metallic Cluster Partitioning in the Nanopore

1. To account for electrode imbalances, set the DC offset voltage such that when the applied potential is set to zero there is no measured current.
2. Prior to adding the POM sample, perform a control experiment to ensure there are no contaminants (*e.g.*, trace POMs from a previous experiment) in the reservoir. Specifically, acquire an ionic current trace under an applied potential of +120 mV to -120 mV in the absence of any POMs to verify that no spontaneous current blockades are present.
   Note: Due to the asymmetric structure of the αHL channel (**Figure 1**), above a critical voltage rectification will be observed and the measured ionic current flowing the channel will differ for positive and negative applied potentials. The ratio of the measured current above this applied voltage is indicative of the orientation of the *α*HL nanopore in the membrane.
3. Add the POM sample by flushing the reservoir with metallic cluster solution at 1 to 5 mM concentration. Alternatively, load the sample into the capillary prior to cell assembly to study the partitioning of POMs into the other end of the αHL channel.
4. Record the ionic current using the manufacturer's software to detect transient current blockades caused by partitioning of individual POMs into the nanopore. Estimate the physical and chemical properties of the molecule from the ionic current blockade depth, event frequency, and the residence time distribution of the blockades.

6. Ion Channel Recordings and Data Analysis

1. Acquire the ionic current time series measurements using a high-impedance, low-noise amplifier and data acquisition system. Perform the measurements at an applied voltage of -120 mV (relative to channel *cis* side) for each pH.
2. Apply a low-pas 100 kHz 8-pole Bessel filter to the signal, which is subsequently digitized at 500 kHz (*i.e.,* 2 ms/point). Extract events from the time series and analyze events using the ADEPT algorithm in the *MOSAIC* software package[32,33].

Representative Results

Over the past two decades, membrane-bound protein nanometer-scale pores have been demonstrated as versatile single-molecule sensors. Such nanopore measurements are conceptually simple: two chambers filled with electrolyte solution are separated by a nanopore embedded in an electrically insulating lipid membrane. Either a patch-clamp amplifier or an external power supply provides an electrostatic potential across the nanopore *via* Ag/AgCl electrodes immersed in the electrolyte reservoirs. The electric field drives individual charged particles into the pore, which produces transient reductions in the ionic current that depend on the size, shape, and charge of the particles. A computer program controls the applied voltage and monitors, in real time, the ionic current blockades caused by molecules reversibly partitioning into the pore. The current is amplified and converted to voltage with a low-noise, high impedance field-effect transistor and digitized using a data acquisition card.

Here, we provide a general procedure for detecting polyoxometalates with a biological nanopore. As seen in **Figure 2**, prior to the addition of POMs the unobstructed channel has a mean open channel current of ~ 100 pA at an applied potential of -120 mV. The addition of POMs produces transient blockades and decreases the ionic current by approximately 80%. As expected, because these particles are negatively charged, the blockades are not observed when the polarity of the applied potential is reversed. Note that if the POMs didn't interact with the pore wall, they would diffuse through the pore's in about 100 ns, which is far too brief to be detected with a conventional patch clamp amplifier. Thus, most of the time a given particle spends in the pore is a direct consequence of the interaction between the particle and the pore. The duration of an ionic current blockade event is defined as the residence time, tau (τ).

To illustrate the utility of this method, we discuss the possibility for an αHL nanopore to monitor the decomposition of 12-phosphotungstic acid (PTA, $H_3PW_{12}O_{40}$) at pH 5.5 and pH 7.5. This decomposition can be observed with ^{31}P NMR measurements, but the concentration needed is 2 mM while nanopore measurements need only 30 μM, because of the sensitivity of the nanopore measurement. At pH 5.5, $[PW_{11}O_{39}]^{7-}$ is the predominant species[30].

The data analysis is performed by calculating a histogram of the relative blockade depth ratio (*i.e.,*$\langle i \rangle/\langle i_o \rangle$, where $\langle i \rangle$ is the mean current with the POM in the pore and $\langle i_o \rangle$ is the mean open channel current). The histogram of the mean current blockade depth ratios at -120 mV and pH 5.5 exhibits a minor peak at $\langle i \rangle/\langle i_o \rangle \approx 0.06$ and major peak at $\langle i \rangle/\langle i_o \rangle \approx 0.16$ (**Figure 3**, *green*). We assume these peaks correspond to $[P_2W_5O_{23}]^{6-}$ and $[PW_{11}O_{39}]^{7-}$, respectively, based on ^{31}P NMR. ^{31}P NMR studies suggest that increasing the pH changes the relative concentration of these two species, and this is borne out by the change in the area of the two peaks shown in **Figure 3**.

When the POM solution is titrated to pH 7.5 *ex situ*, the total POM concentration decreases due to the partial degradation of the two-principal species to inorganic salts(*i.e.,* free phosphate, $H_xPO_4^{-3+x}$ and tungstate, WO_4^{2-} ions). The histogram of the relative blockade depth ratio also shows two principal peaks (**Figure 3**, *orange*), but with 20-fold fewer events (which suggests the total POM concentration at pH 7.5 is approximately 20-fold less than that at pH 5.5, if the nanopore's capture efficiency for POMs is the same at the two pH values). It is interesting to note that at pH 7.5 and greater, the POM species observed here were not detected in the ^{31}P NMR spectrum due to their low concentration caused by their dissociation into phosphate and tungstate ions.

Each event's residence time in the pore is defined by the duration of the individual ionic current blockades. The distribution of residence times provides insight into the different species that are present. It was shown earlier that for blockades caused by a differently-sized polymers of poly(ethylene glycol), the residence time distribution for each size of that polymer is well described by a single exponential. That result suggests the interaction of that polymer is a simple reversible chemical reaction[12,13,20].

Copyright © 2018 Journal of Visualized Experiments

Figure 4 illustrates that the residence time distributions for the two peaks were well differentiated at pH 5.5 and 7.5. Two features are clear. First, under all conditions, multiple exponentials are required to fit each of the distributions, which suggests there are variations of the POMs within each species. Second, the residence times of the POMs in the pore are much shorter at pH 7.5 compared to those at pH 5.5, which suggests a weakening of the interaction between the pore and POMs. It has been shown previously that a change in pH alters the relative number of fixed charges in or near the *α*HL channel lumen. These changes will directly alter the interactions with partitioning POMs inside the pore and therefore modify their residence times[34,35].

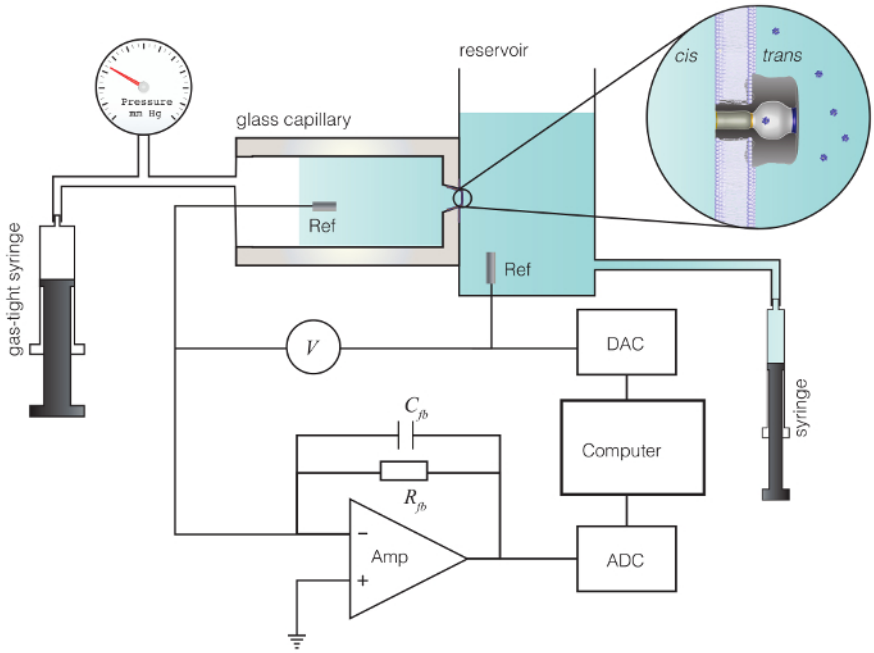

Figure 1: Schematic diagram of the experimental setup. Method for nanopore-based characterization of individual polyoxometalate molecules. A protein nanopore that self-assembles in a 4 nm thick lipid bilayer membrane is bathed by aqueous electrolyte solutions in a glass capillary and larger reservoir. A pressure is applied to the glass capillary with a gas tight syringe to aid nanopore incorporation. A potential *V* is applied across the membrane with a matched pair of Ag/AgCl electrodes and drives an ionic current (*e.g.*, Na^+ and Cl^-) through the pore. The current is converted to voltage with a high impedance amplifier, digitized with an analog to digital converter (ADC) and stored on a computer. Computer software controls the applied potential through a digital to analog converter (DAC) and monitors, in real time, the transient current blockades caused by single molecules that partition into the pore. Please click here to view a larger version of this figure.

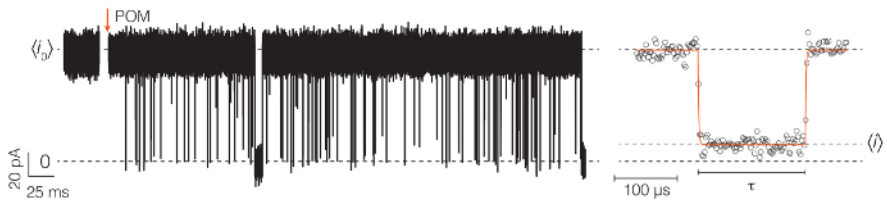

Figure 2: Nanopore-based detection of individual metallo-nanoparticles. An illustration of ionic current time series traces that occur before and after the addition of a POM solution to the nanopore apparatus. The partitioning of individual anionic POMs into the pore causes transient current reductions in the mean open pore current, $\langle i_o \rangle$. (*Right*) A typical event, illustrating the mean current of the blockade ($\langle i \rangle$) and the residence time (τ) of the particle in the pore. The applied potential was -120 mV, and the solutions contained 1 M NaCl, 10 mM NaH_2PO_4 at pH 5.5. The cis compartment also contained 30 µM of 12-phosphotungstic acid. The current blockade depth ratio ($\langle i \rangle / \langle i_o \rangle$) and the residence times (τ) provide information about which POM species are present in solution. Under the conditions we used here, the αHL channel does not gate (spontaneously close) when POMs are not present. *Please click here to view a larger version of this figure.*

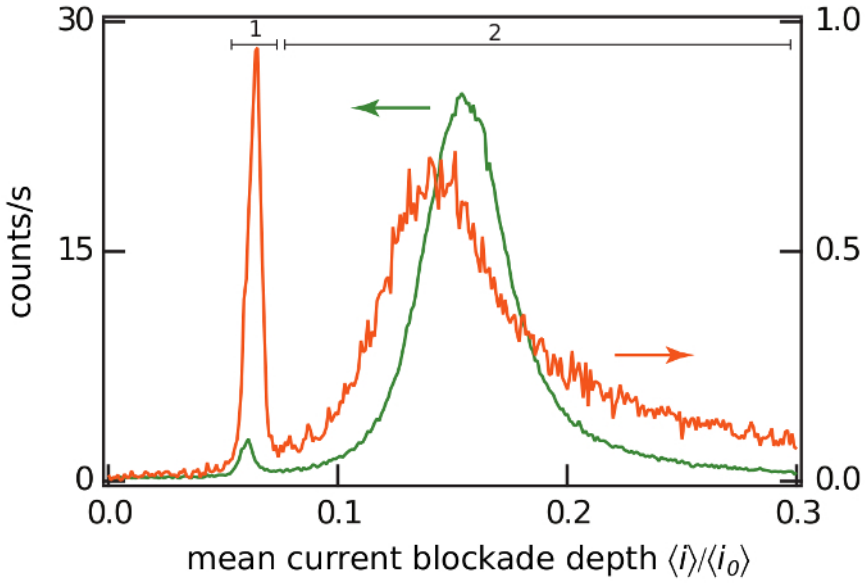

Figure 3: Histograms of the current blockade depth ratio at pH 5.5 and 7.5. Histograms of the POM-induced ionic current blockade depth ratio at pH 5.5 (*green*) and 7.5 (*orange*) with an applied potential V = -120 mV. The two peaks present at each pH value correspond to the known predominate POM species in solution under those conditions. The current blockade depth ratios of 0 and 1 correspond to a fully blocked and open pore, respectively. The histograms were created with a bin width of 0.001 and normalized to counts/s by dividing by the data acquisition time. Please click here to view a larger version of this figure.

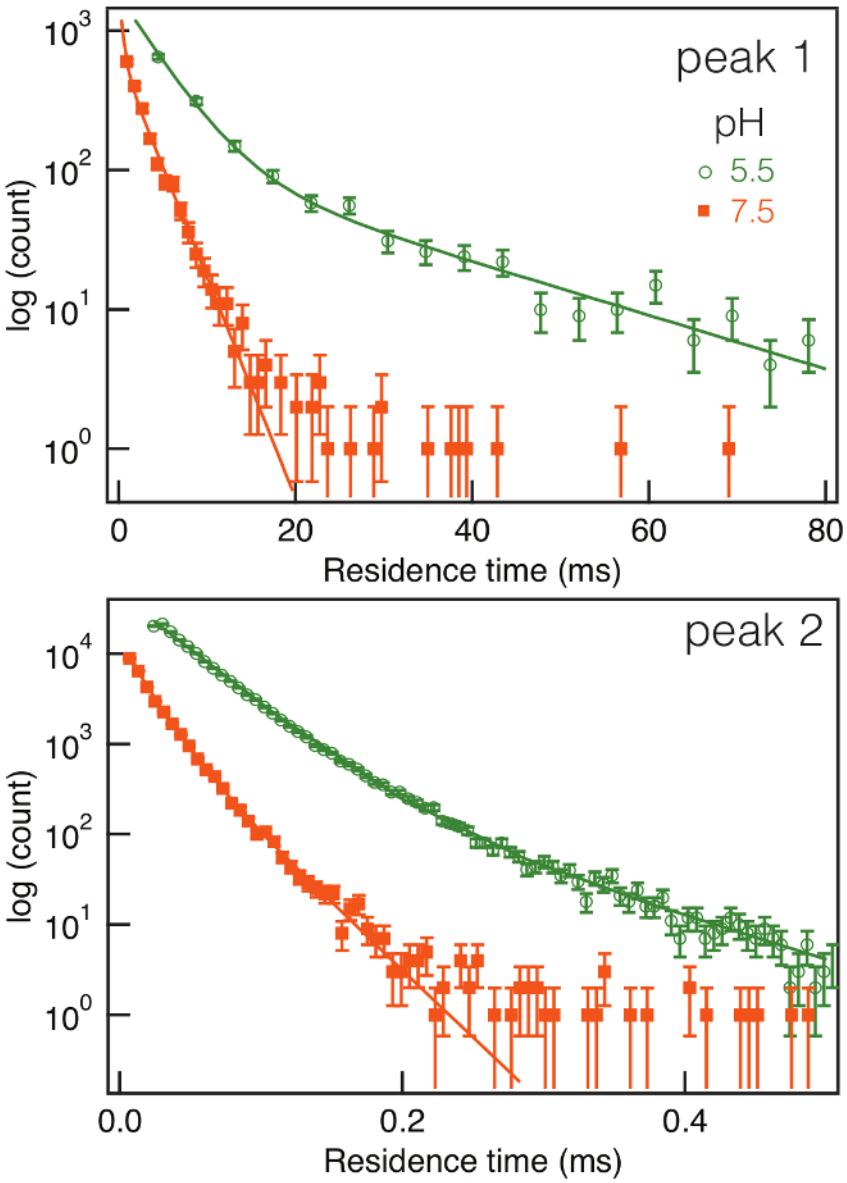

Figure 4: Residence time distribution and fitting with several exponentials. The distribution of residence times for POM-induced current blockades caused by the two-principal species (peaks 1 and 2 in **Figure 4**) observed at pH 5.5 and 7.5 in a semi-log plot. For both species, the residence times are markedly shorter at the higher pH value, which suggests the interaction between the pore and POMs changed. The solid lines are fits of an exponential mixture model to the data. Please click here to view a larger version of this figure.

Discussion

Due to their anionic charge, POMs likely associate with organic counter cations through electrostatic interactions. Therefore, it is important to identify the proper solution conditions and the right electrolyte environments (especially cations in solution) to avoid complex formation with POMs. Particular care is required in the buffer choice. For example, the capture rate of POMs with tris(hydroxymethyl)aminomethane and citric acid-buffered solutions is significantly lower than that in phosphate buffered solution, likely because the first two buffers form a complex with the POM that doesn't strongly interact with the nanopore. Moreover, the NaCl electrolyte was purposely used instead of KCl (as well as the other alkali metals) to avoid the precipitation of $[PW_{11}O_{39}]^{7-}$ by K^{+}.

Critical to the accurate measurement of the residence time distributions is the ability to measure the current at a sufficiently high bandwidth. For instance, with exponentially-distributed residence times there are far more blockades with short than long residence times, and an accurate estimation of the residence time distributions is better achieved by collecting a great deal of data (*i.e.,* acquiring it at as high as a bandwidth the system's electrical capacitance allows). To achieve this condition in nanopore spectroscopy, the system capacitance (membrane and stray capacitance) should be minimized. Stray capacitance is reduced by decreasing the length of all connecting cables and using high quality electrical contacts. The membrane capacitance is minimized by decreasing the surface area of the bilayer membrane, increasing the thickness of supporting materials (*i.e.,* quartz, polytetrafluoroethylene, *etc.*), and decreasing the area of exposed supporting materials to the electrolyte. In practice, a typical instrument's stray capacitance (≈ 2 pF) will limit the noise for membranes < 1 to 5 m in diameter. This constitutes the method's

limitation. For example, the detection of small and highly charged single molecules can be challenging due to their relatively short residence time.

The mechanism by which pressure enables control of channel insertion is not completely understood. The quartz microcapillaries have a very small diameter on which the membrane is formed. Applying pressure will cause the membrane to bulge (thereby increasing the membrane surface area) and possibly thin the membrane. Both effects would increase the rate at which channels will form in the membrane. When a single channel spontaneously forms, reduce the pressure to prevent the insertion of additional channels. The removal of non-inserted HL from the bulk aqueous phase is not required if the *α*HL concentration is sufficiently low.

The structures and charges of polyoxometalates are currently studied using traditional analytical chemistry techniques, including NMR, Ultraviolet-visible, Infrared and Raman spectroscopy, mass spectrometry, and X-ray diffraction. We expect that nanopore measurements will complement the characterization of these and other physical properties of POMs, as well as the study of their speciation at low concentration, which will help better understand the synthetic pathway of polyoxometalates formation. It was also shown previously that the *α*HL pore can even distinguish between 2 isomers of the trivacant Keggin form $Na_8HPW_9O_{34}$[30].

In summary, we have shown that a membrane-bound protein nanopore can be used to detect and characterize tungsten oxide metallic clusters (heteropolytungstates) in solution using a simple high-resolution electrical measurement. The sensitivity afforded by this novel approach permits the tracking of subtle differences in POM structure that arise at different pH values at concentrations that are substantially lower (> 70-fold) than required for traditional methods such as NMR spectroscopy. Due to the single molecule detection capability of nanopores, the actual limit of detection in the method can be made much lower by measuring the current for longer times (the capture rate scales in proportion to the POM concentration).

Disclosures

None.

Acknowledgements

We are grateful for financial support from the European Molecular Biology Organization for a postdoctoral fellowship (to J.E.) and a grant from the NIH NHGRI (to J.J.K.). We appreciate the help of Professors Jingyue Ju and Sergey Kalachikov (Columbia University) for providing heptameric αHL, and for inspiring discussions with Professor Joseph Reiner (Virginia Commonwealth University).

References

1. Ettedgui, J., Kasianowicz, J. J., & Balijepalli, A. Single molecule discrimination of heteropolytungstates and their Isomers in solution with a nanometer-scale pore. *Journal of the American Chemical Society.* **138** (23), 7228-7231 (2016).
2. Bezrukov, S., & Kasianowicz, J. Current noise reveals protonation kinetics and number of ionizable sites in an open protein ion channel. *Physical Review Letters.* **70** (15), 2352-2355 (1993).
3. Kasianowicz, J. J., & Bezrukov, S. M. Protonation dynamics of the alpha-toxin ion channel from spectral analysis of pH-dependent current fluctuations. *Biophysj.* **69** (1), 94-105 (1995).
4. Please, T. R., & Ayub, M. *Solid-State Nanopore. Engineered Nanopores for Bioanalytical Applications.*, 121-140 Elsevier Inc. (2013).
5. Dekker, C. Solid-state nanopores. *Nature Nanotechnology.* **2** (4), 209-215 (2007).
6. Kasianowicz, J. J., Brandin, E., Branton, D., & Deamer, D. W. Characterization of individual polynucleotide molecules using a membrane channel. *Proceedings of the National Academy of Sciences of the United States of America.* **93** (24), 13770-13773 (1996).
7. Akeson, M., *et al.* Microsecond time-scale discrimination among polycytidylic acid, polyadenylic acid, and polyuridylic acid as homopolymers or as segments within single RNA molecules. *Biophysical Journal.* **77** (6), 3227-3233 (1999).
8. Singer, A., & Meller, A. Nanopore-based Sensing of Individual Nucleic Acid Complexes. *Israel Journal of Chemistry.* **49** (3-4), 323-331 (2010).
9. Jin, Q., Fleming, A. M., Burrows, C. J., & White, H. S. Unzipping kinetics of duplex DNA containing oxidized lesions in an α-hemolysin nanopore. *Journal of the American Chemical Society.* **134** (26), 11006-11011 (2012).
10. Halverson, K. M., *et al.* Anthrax biosensor, protective antigen ion channel asymmetric blockade. *Journal of Biological Chemistry.* **280** (40), 34056-34062 (2005).
11. Oukhaled, G., *et al.* Unfolding of proteins and long transient conformations detected by single nanopore recording. *Physical Review Letters.* **98** (15), 158101 (2007).
12. Reiner, J. E., Kasianowicz, J. J., Nablo, B. J., & Robertson, J. W. F. Theory for polymer analysis using nanopore-based single-molecule mass spectrometry. *Proceedings of the National Academy of Sciences of the United States of America.* **107** (27), 12080-12085 (2010).
13. Robertson, J. W. F., *et al.* Single-molecule mass spectrometry in solution using a solitary nanopore. *Proceedings of the National Academy of Sciences of the United States of America.* **104** (20), 8207-8211 (2007).
14. Baaken, G., Ankri, N., Schuler, A.-K., Rühe, J., & Behrends, J. C. Nanopore-based single-molecule mass spectrometry on a lipid membrane microarray. *ACS Nano.* **5** (10), 8080-8088 (2011).
15. Angevine, C. E., Chavis, A. E., Kothalawala, N., Dass, A., & Reiner, J. E. Enhanced single molecule mass spectrometry *via* charged metallic clusters. *Analytical Chemistry.* **86** (22), 11077-11085 (2014).
16. Astier, Y., Uzun, O., & Stellacci, F. Electrophysiological study of single gold nanoparticle/alpha-Hemolysin complex formation: a nanotool to slow down ssDNA through the alpha-Hemolysin nanopore. *Small.* **5** (11), 1273-1278 (2009).
17. Chavis, A. E., Brady, K. T., Kothalawala, N., & Reiner, J. E. Voltage and blockade state optimization of cluster-enhanced nanopore spectrometry. *Analyst.* **140** (22), 7718-7725 (2015).
18. Campos, E., *et al.* Sensing single mixed-monolayer protected gold nanoparticles by the α-hemolysin nanopore. *Analytical Chemistry.* **85** (21), 10149-10158 (2013).

Copyright © 2018 Journal of Visualized Experiments

19. Campos, E., *et al.* The role of Lys147 in the interaction between MPSA-gold nanoparticles and the α-hemolysin nanopore. *Langmuir.* **28** (44), 15643-15650 (2012).
20. Baaken, G., *et al.* High-Resolution Size-Discrimination of Single Nonionic Synthetic Polymers with a Highly Charged Biological Nanopore. *ACS Nano.* **9** (6), 6443-6449 (2015).
21. Berzelius, J. J. Beitrag zur näheren Kenntniss des Molybdäns. *Annalen Der Physik.* **82** (1), 369-392 (1826).
22. Long, D.-L., Burkholder, E., & Cronin, L. Polyoxometalate clusters, nanostructures and materials: from self assembly to designer materials and devices. *Chemical Society Reviews.* **36** (1), 105-121 (2007).
23. Muller, A., *et al.* Polyoxovanadates: High-nuclearity spin clusters with interesting host-guest systems and different electron populations. Synthesis, spin organization, magnetochemistry, and spectroscopic studies. *Inorganic Chemistry.* **36** (23), 5239-5250 (1997).
24. Rausch, B., Symes, M. D., Chisholm, G., & Cronin, L. Decoupled catalytic hydrogen evolution from a molecular metal oxide redox mediator in water splitting. *Science.* **345** (6202), 1326-1330 (2014).
25. Dolbecq, A., Dumas, E., Mayer, C. R., & Mialane, P. Hybrid organic-inorganic polyoxometalate compounds: from structural diversity to applications. *Chemical Reviews.* **110** (10), 6009-6048 (2010).
26. Busche, C., *et al.* Design and fabrication of memory devices based on nanoscale polyoxometalate clusters. *Nature.* **515** (7528), 545-549 (2014).
27. Pope, M., & Müller, A. *Polyoxometalates: From Platonic Solids to Anti-Retroviral Activity.* **10** Springer Science & Business Media: Dordrecht (2012).
28. Rhule, J. T., Hill, C. L., Judd, D. A., & Schinazi, R. F. Polyoxometalates in medicine. *Chemical Reviews.* **98** (1), 327-358 (1998).
29. Gao, N., *et al.* Transition-metal-substituted polyoxometalate derivatives as functional anti-amyloid agents for Alzheimer's disease. *Nature Communications.* **5**, 3422 (2014).
30. Pope, M. T. *Heteropoly and Isopoly Oxometalates.* **8** Springer-Verlag Berlin Heidelberg (1983).
31. Braha, O., *et al.* Designed protein pores as components for biosensors. *Chemistry & Biology.* **4** (7), 497-505 (1997).
32. Forstater, J. H., *et al.* MOSAIC: A modular single-molecule analysis interface for decoding multistate nanopore data. *Analytical Chemistry.* **88** (23), 11900-11907 (2016).
33. Balijepalli, A., *et al.* Quantifying Short-Lived Events in Multistate Ionic Current Measurements. *ACS Nano.* **8**, 1547-1553 (2014).
34. Misakian, M. M., & Kasianowicz, J. J. J. Electrostatic influence on ion transport through the alphaHL channel. *Journal of Membrane Biology.* **195** (3), 137-146 (2003).
35. Piguet, F., *et al.* Identification of single amino acid differences in uniformly charged homopolymeric peptides with aerolysin nanopore. *Nature Communication.* **9** (966) (2018).

Copyright © 2018 Journal of Visualized Experiments